Glass Physics and Chemistry, Vol. 31, No. 1, 2005, pp. 44–52.

PROCEEDINGS OF THE THIRD RUSSIAN–ISRAELI BI-NATIONAL WORKSHOP 2004 "THE OPTIMIZATION OF THE COMPOSITION, STRUCTURE, AND PROPERTIES OF METALS, OXIDES, COMPOSITES, NANOMATERIALS, AND AMORPHOUS MATERIALS"

(St. Petersburg, Russia, June 13–23, 2004)

Extruded High-Strength Solid Materials Based on Magnesium with Zinc, Yttrium, and Cerium Additives

X. Guo* and D. Shechtman**

** School of Materials Science and Engineering, University of Technology, Xi'an, 710048 China*

*** Department of Materials Engineering, Israel Institute of Technology (Technion), Technion City, Haifa, 32000 Israel*

e-mail: mtrdan@techunix.technion.ac.il

Abstract—Magnesium (the lightest structural material) is suitable for manufacturing movable parts of vehicles and finds wide application in car and aerospace engineering. Magnesium alloys produced by conventional casting have defects and large-sized grains and exhibit undesirable mechanical properties. The desirable properties of magnesium alloys can be achieved by improving their microstructure. This paper reports on the results of investigations of high-strength products (8–50 mm in diameter) prepared by extrusion from rapidly solidified ribbons of the Mg–6Zn–1.5Y–0.5Ce alloy (hereafter, numbers in the compositions indicate the elemental content in wt %). The tensile strengths of the products are equal to 450–520 MPa, and their elongation (E, %) is limited. The microstructure of the materials at each stage of treatment is examined using optical microscopy or scanning electron microscopy with energy-dispersive X-ray analysis and X-ray diffraction. It is demonstrated that Mg–Zn–Y–Ce alloys with a fine-grained structure can be prepared by both conventional casting and rapid solidification. The mean sizes of magnesium solid-solution grains and supersaturated magnesium solid-solution grains are equal to 45 and 5 μm for alloys produced by casting and rapid solidification, respectively. The formation of a fine-grained structure is predominantly associated with the remelting of solidified dendrites. In this process, cerium plays a decisive role. The theoretically expected tensile yield strength of the Mg–6Zn–1.5Y–0.5Ce high-strength solid materials produced by extrusion should be higher for materials with a fine-grained structure. It is shown that the discrepancy between the theoretical and experimental results is caused by the extrusion defects. The conclusion is drawn that the strength of the materials extruded from rapidly solidified ribbons depends on their microstructure and extrusion conditions.

INTRODUCTION

Magnesium–zinc alloys with additives of yttrium and other rare-earth elements belong to an important group of materials in the magnesium alloy family [1–5] and possess good mechanical properties at both elevated and room temperatures [6]. However, the possibilities of producing alloys with a finer microstructure and better mechanical properties are limited by the properties of their Mg–Zn master alloys. Magnesium alloys prepared by conventional casting, as a rule, have large-sized defects and coarse grains, including pores, microstructural inhomogeneities, and inclusions formed upon oxidation [6]. This leads to a deterioration of the mechanical and chemical properties (such as the rigidity, strength, elongation, and corrosion resistance) at ambient or high temperatures. In particular, for materials produced by conventional casting, the tensile strength is lower than 300 MPa, the elongation is less than 20%, and the secondary creep strength is lower than that of aluminum alloys [6].

The necessity of improving the quality of materials has given impetus to the design of new magnesium alloys with a finer microstructure and better mechanical properties. Zirconium has been widely used to improve the mechanical properties of Mg–Zn alloys [1. 6]. However, the mean size of grains in such alloys is equal to several tens of micrometers. This is far from the desired size, because a tensile strength higher than 400 MPa can be achieved by decreasing the grain size to several micrometers [7]. The synthesis of fine-grained materials provides a means for improving their mechanical properties and reducing microsegregation. In turn, this results in a higher corrosion resistance. Therefore, the decrease in the degree of granularity is a key factor that makes it possible to extend the field of application of Mg–Zn alloys for products of aircraft and space engineering.

Compared to the conventional casting, the rapid solidification provides better alloying and, hence, the formation of a finer microstructure, which, in turn, improves the mechanical and physical properties of alloys in different metal systems [8, 9]. A number of attempts have been made to use rapid solidification in the design and study of magnesium alloys [9]. It should

1087-6596/05/3101-0044 © 2005 Pleiades Publishing, Inc.

be noted that there are many works dealing with the preparation of magnesium alloys with a tensile strength of higher than 400 MPa. However, only a few works have been concerned with the study of the microstructure in the course of solidification, including grain refinement and mechanisms of strengthening. The purpose of the present work was to prepare ribbons from the Mg–Zn, Mg–Zn–Y, and Mg–Zn–Ce alloys by the rapid solidification method, to explain the improvement of their microstructure, and to measure the mechanical properties of extruded solid materials produced from these rapidly solidified ribbons.

SAMPLE PREPARATION AND EXPERIMENTAL TECHNIQUE

Alloys of compositions Mg–6Zn, Mg–6Zn–1.5Y, and Mg–6Zn–1.5Y–1Ce were prepared from the Mg–47Y, Mg–90Ce, 99.9Mg, and 99.9Zn master alloys in a resistance furnace (hereafter, numbers in the compositions indicate the elemental content in wt %). All the alloys before and after melting were analyzed on an energy-dispersive X-ray spectrometer. The melting was performed at a temperature of 760°C in graphite crucibles. During melting, the melts were covered with a mixture of fluxes consisting of 50% KCl and 50% NaCl or protected with a mixture of argon and SF_6 gases. Cylindrical ingots 22 mm in diameter and 110 mm in length were produced by casting into carbon steel molds. Ribbons 3 mm wide and 80 μm thick were fabricated by remelting the Mg–6Zn, Mg–6Zn–1.3Y, and Mg–6Zn–1.5Y–0.5Ce ingots with the use of a single-roller melt spinning apparatus in an argon atmosphere. The melt at a temperature of approximately 700°C was poured onto the surface of a spinning cooper wheel.

The ribbons were powdered, and the powders obtained were stored in a protective atmosphere prior to compaction and extrusion. The diameter of extruded solid products varied from 8 to 50 mm. The ribbons were analyzed on a Philips X-ray diffractometer (CuK_α radiation, 40 kW, 40 μA).

For microstructural examination, the ribbons were edge-mounted (along the longitudinal cross section) in a self-curing resin. All the samples taken at each experimental stage were polished to 1 μm, etched in a 5% HNO_3 solution in ethanol, examined under an Axiophot optical microscope with a digital system, coated with carbon, and analyzed on a Philips XL 30 scanning electron microscope (SEM) equipped with an Oxford Link ISIS energy-dispersive X-ray spectrometer. The samples for measurements of the tensile strain were prepared from the extruded solid products of different diameters. The length of a gauge was equal to 30 mm. The sample diameter was 6 mm. The tension experiments were carried out at room temperature on a computer-controlled tensile tester. The speed of a slider was equal to 1 mm/min, and the strain rate was 5.5×10^{-3} s^{-1}.

RESULTS

Microstructure of Alloys Prepared by Conventional Solidification

Figure 1 shows the microstructures of the alloys produced by the conventional solidification. The microstructures of the Mg–6Zn (Figs. 1a, 1b) and Mg–6Zn–1.5Y (Figs. 1c, 1d) alloys contain coarse dendritic grains (solidifying first) surrounded by the eutectic material. The coarse dendritic grains in both alloys are similar to each other. The microstructure of the Mg–6Zn–1.5Y–1Ce alloy (Figs. 1e, 1f) also consists of magnesium and eutectics. Examination of the microstructures in different cross sections revealed that magnesium is contained in all small-sized grains whose sizes are approximately equal to 45 μm (Fig. 1e). This is approximately equal to the width of dendrite arms in the Mg–6Zn or Mg–6Zn–1.5Y alloys (Figs. 1a, 1c). Consequently, cerium most likely plays an important role in the decrease in the size of grains in the Mg–Zn–Y–Ce alloy. Moreover, it is possible to assume that the grains of the Mg–Zn–Y–Ce alloy are formed from the dendrite arms grown in the course of solidification.

According to the energy-dispersive X-ray analysis, the eutectic compounds contain 30 at. % Zn in the Mg–Zn alloy; 37.6 at. % Zn and 7.4 at. % Y in the Mg–Zn–Y alloy; and 34 at. % Zn, 14.5 at. % Y, and 2.5 at. % Ce in the Mg–Zn–Y–Ce alloy. The distributions of alloy elements inside dendrite arms or grains are shown in Fig. 2. It can be seen from this figure that yttrium has a limited solubility in magnesium and cerium is almost insoluble in magnesium. As a consequence, both yttrium and cerium precipitate at the grain boundaries and form a compound.

Microstructure of Ribbons

As follows from the X-ray diffraction patterns depicted in Fig. 3, the Mg–Zn alloys contain only the supersaturated magnesium solid solution. The Mg–Zn–Y alloys involve the supersaturated magnesium solid solution, the $Mg_3Y_2Zn_3$ (W) phase (in small amounts), and compounds corresponding to two or three unidentified peaks at small angles. The Mg–Zn–Y–Ce alloy is composed of the supersaturated magnesium solid solution and the W and $Mg_{17}Ce_2$ phases.

The microstructures of these rapidly solidified alloys are depicted in Fig. 4. In the Mg–Zn alloy (Fig. 4a), the microstructure is formed by irregular grains with a diameter ranging from 10 to 50 μm. The grains closer to the quenching surface are coarser than those closer to the freely cooled surface. This suggests that, first, the copper cooler (wheel) has no catalytic effect on the crystallization of the alloys under consideration and, second, the structure of the copper lattice (face-centered cubic lattice) differs from the structure of the lattice of the initial supersaturated magnesium solid solution (hexagonal close-packed lattice).

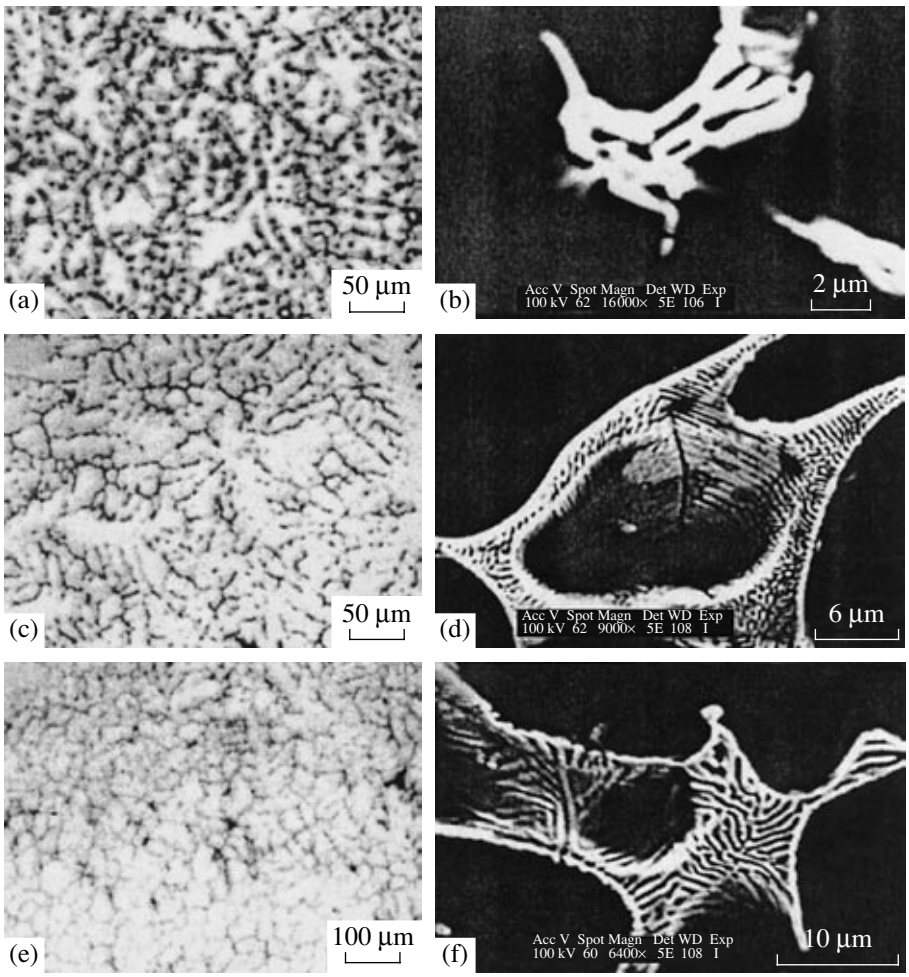

Fig. 1. Microstructures of (a, b) Mg–6Zn, (c, d) Mg–6Zn–1.5Y, and (e, f) Mg–6Zn–1.5Y–1Ce alloys prepared by conventional solidification.

The microstructure of the Mg–Zn–Y ribbon involves grains of the supersaturated magnesium solid solution, submicroparticles, and networks comprised of boundary grains. The submicroparticles are uniformly distributed in the grains of the supersaturated magnesium solid solution. These grains are formed in two different layers along the cross section. The layer adjacent to the quenched surface consists of columnar grains from 10 to 20 μm in length and from 5 to 10 μm in width. The axes of these grains are perpendicular to the solidification front rather than to the quenched surface. The layer bordering the columnar grains has a fine-grained structure with a mean grain diameter of approximately 5 μm. Isolated intermetallic compounds decorate the grain boundaries.

It was found that an increase in the yttrium content from 1.3 to 3.2 wt % does lead to a substantial difference between the Mg–6Zn–1.3Y and Mg–6Zn–3.2Y alloys. The sizes, shapes, and distributions of submicroparticles in the Mg–Zn–Y and Mg–Zn–Y–Ce alloys are similar to each other.

The microstructure of the Mg–Zn–Y–Ce alloy consists of irregular grains with a mean diameter of 5 μm, submicroparticles inside the grains, and continuous networks at the grain boundaries (Figs. 4e, 4f). The density of submicroparticles is higher in regions closer to the quenched surface.

According to the energy-dispersive X-ray analysis, the Mg–Zn–Y and Mg–Zn–Y–Ce alloys are supersaturated with Zn and Y. In the Mg–Zn–Y–Ce alloy, the cerium content in a number of submicroparticles and continuous networks is higher than the mean content in the alloy. As follows from the X-ray diffraction data, this is associated with the formation of the $Mg_{17}Ce_2$ phase. Moreover, it was revealed that cerium can be located only in particular regions, whereas other regions of grains do not contain cerium at all. In order to confirm this finding, we analyzed the cerium distribution in the inner grains by using the energy-dispersive spectrometer with a linear scanner and obtained the same results (Fig. 5). This suggests that, most likely, cerium does not dissolve at all in the supersaturated

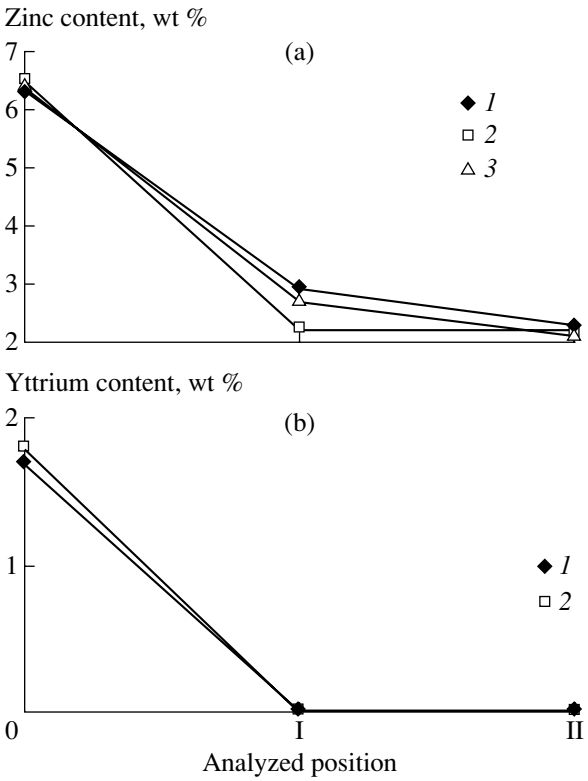

Fig. 2. (a, b) Distributions of elements inside the dendrite arms or grains in (*1*) Mg–6Zn, (*2*) Mg–6Zn–1.5Y, and (*3*) Mg–6Zn–1.5Y–1Ce according to the energy-dispersive X-ray analysis in positions 0 (near the surface of dendrite arms), I (between positions 0 and II), and II (in the vicinity of the center of dendrite arms).

magnesium solid solution under our experimental conditions. All cerium enters into the composition of intermetallic compounds in the form of submicroparticles or networks.

Microstructure and Mechanical Properties of As-Extruded Solid Materials

We investigated the microstructure of the as-extruded samples. Furthermore, we studied the fractured surface of the samples ruptured under tension. The Mg–Zn–Y–Ce extruded samples of different diameters have similar microstructures (except for insignificant differences between the compositions of different melt spinning batches).

In the course of extrusion, the grains are rotated and elongated. This provides preferred crystallographic orientations, i.e., the formation of an extended texture. As can be seen from Fig. 6, the eutectic grains are broken and uniformly dispersed in the matrix. These dispersed particles substantially affect the mechanical properties of the extruded materials. It can be seen from Fig. 6 that there are a number of welding defects between dispersed powder particles.

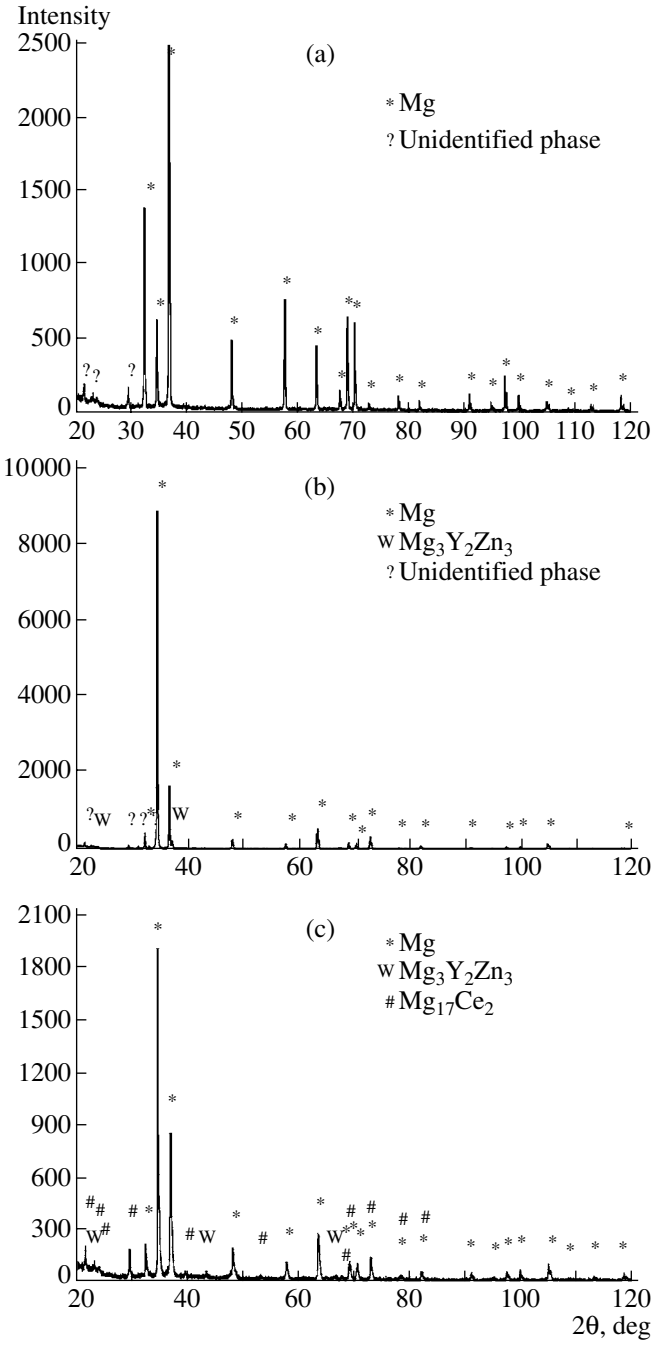

Fig. 3. X-ray diffraction patterns of (a) Mg–6Zn, (b) Mg–6Zn–1.3Y, and (c) Mg–6Zn–1.5Y–0.5Ce alloys.

The SEM images of the samples ruptured under tension are displayed in Fig. 7. It can be seen from this figure that the fractures are dimpled, which is characteristic of ductile fracture. Particles can be observed at the dimple bottom.

Mechanical testing of the alloys revealed that the tensile strength of our alloys varies from 490 to 520 MPa and that their elongation ability is limited.

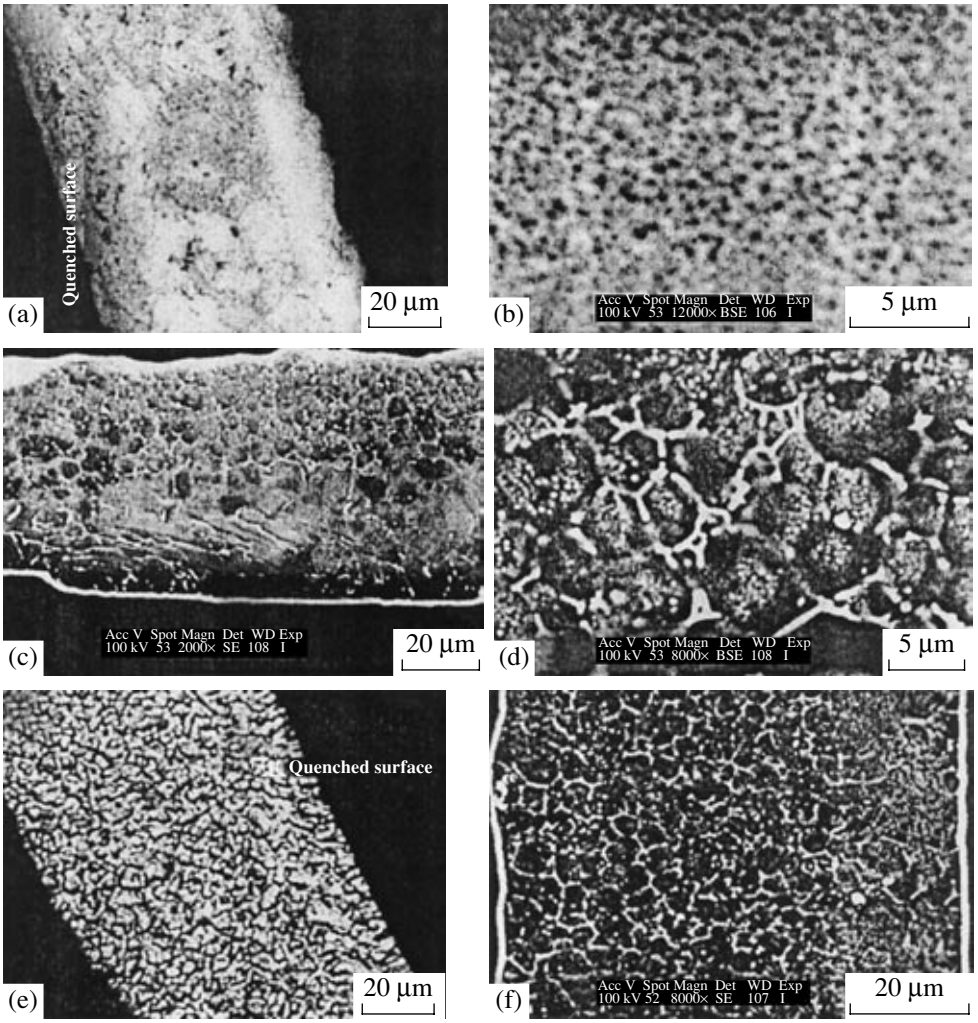

Fig. 4. Microstructures of (a, b) Mg–6Zn, (c, d) Mg–6Zn–1.3Y, and (e, f) Mg–6Zn–1.5Y–0.5Ce alloys prepared by rapid solidification.

DISCUSSION

Improvement of the Grain Structure of the Mg–Zn–Y–Ce Alloy Prepared by Conventional Solidification

It is well known that the dendrite growth is accompanied by remelting of dendrite arms. During the growth, dendrite arms can split off from the trunk [10]. The energy-dispersive X-ray analysis performed in the present work demonstrates that yttrium and cerium due to their limited solubility in the magnesium solid solution [11] are predominantly accumulated at the grain boundaries. Consequently, the redistribution of yttrium and cerium in the melt toward arm necks in the course of solidification should favor the detachment of the arms. In particular, all cerium should diffuse into the liquid in the vicinity of the solid–liquid interface, be accumulated in arm necks, and promote the remelting at points of joining arms and trunks. Under the action of a driving force, namely, the surface energy, the thickness of arm necks decreases, the arms split off from the trunks, and, eventually, the arms transform into grains during subsequent solidification. Therefore, the insolubility of cerium plays a decisive role in the formation of a finer grained structure of the Mg–Zn–Y–Ce alloys.

Improvement of the Grain Structure of Mg–Zn–Y–Ce Ribbons

The solute trapping [12] results in the formation of the supersaturated magnesium solid solution in the ribbons during rapid solidification. According to the modern theory of nonequilibrium solidification [13] and the experimental results obtained by Willnecker *et al.* [14], coarser grains consisting of considerably finer dendrite arms should be formed with an increase in the solidification rate. As a consequence, in the Mg–Zn and Mg–Zn–Y alloys, grains in the vicinity of the quenched surface are coarser than those located in the vicinity of the freely cooled surface owing to the quenching. In the

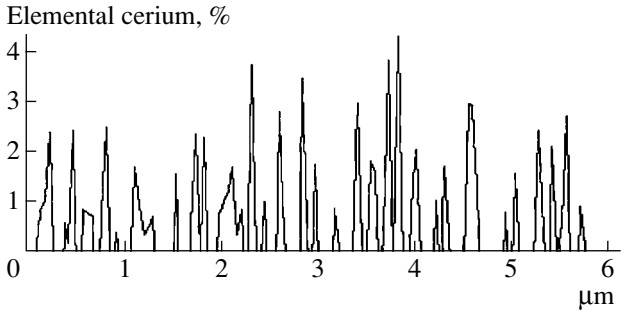

Fig. 5. Cerium distribution across the grain in a rapidly solidified ribbon of the Mg–6Zn–1.5Y–0.5Ce alloy according to the scanning energy-dispersive X-ray analysis.

Mg–Zn–Y–Ce alloy, fine homogeneous grains are formed along the cross section of the ribbons. Therefore, the improvement of the grain structure correlates with the cerium content and the microstructures of the Mg–Zn–Y and Mg–Zn–Y–Ce alloys differ from each other. The formation of a finer structure can be explained in terms the remelting mechanism [15].

Rapid solidification is a nonequilibrium process involving two sequential stages for metals upon supercooling [13–15]. At the first stage, the material solidifies rapidly and coarse grains containing very fine supersaturated dendrite arms (cellular structure) are formed from a melt that is strongly supercooled as a result of quenching. The formation of the dendrite arms is attended by the liberation of the latent heat and the temperature recalescence. At the second stage, the fine dendrite arms are superheated and can be partially remelted or broken as a result of abrupt shrinkage and (or) melt flow. At this stage, the fraction of the solidified melt amounts to only 20% of the total melt [16]. After rapid solidification, the residual melt undergoes conventional solidification. The remelting of the fine dendrite arms gives way to progressive melting with the redistribution of the solute and the heat flux. The solute trapping leads to a decrease in the solidus and liquidus temperatures. The supersaturated coarse grains can disaggregate into small-sized dendritic segments or groups, because the superheating depends on the solidification time at a particular point, the accumulation of the solute around arm necks due to the solute redistribution, and the heat flux [15]. In rapidly solidified ribbons, the local solidification time is limited by a large surface-to-volume ratio. The accumulation of the solute and the heat flux are decisive factors and, hence, predominantly determine whether or not the fine arms will be partially remelted and the coarse grains will disaggregate into small-sized dendritic segments. In the Mg–6Zn–1.3Y alloy, the amount of the accumulated solute around the dendrite arm necks on the quenched surface is not large enough for the arms to be remelted and the coarse grains formed at the first stage can retain their dendrite skeletons in the course of the solidification process. On the other hand, the dendrite arms of the coarse grains on the freely cooled surface can be partially remelted and disaggregate into small-sized dendritic segments. Subsequently, these segments grow in the residual melt and displace the solute to the solid–liquid front. Finally, the enriched melt around segments solidifies to form anomalous eutectics, because the amount of the melt is limited. The eutectic magnesium solid solution transforms into the primary supersaturated magnesium solid solution, and the intermetallic compounds are formed in the network around the grains.

It is revealed that the desegregation depends substantially on the rate of solidification or supercooling of the melt. In the case when the rate of solidification or supercooling of the melt is higher than the critical value, the disaggregation can be partially or completely suppressed and the coarse grains are retained in the vicinity of the quenched surface (Fig. 4c). Otherwise, if the rate of solidification or supercooling of the melt is lower than the critical value, the coarse dendritic grains are formed, as is the case with conventional casting. The analysis of the experimental data permits us to make the inference that the magnesium ribbons undergo destruction during rapid solidification. On the freely cooled surface (Fig. 2b), the rates of solidification or supercooling of the melts are most likely high enough for the fine microstructure of alloys in the Mg–

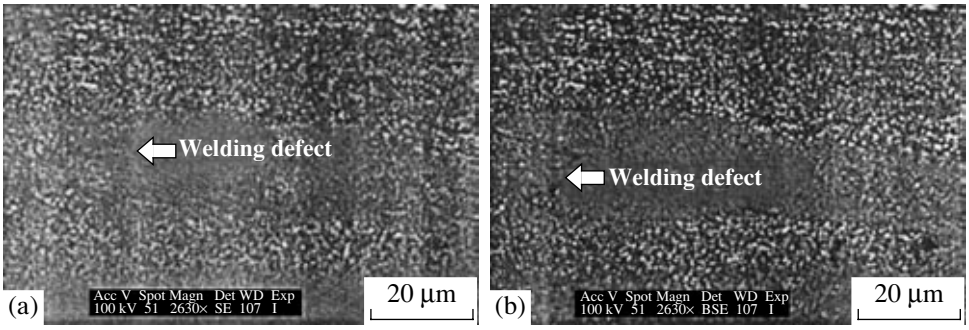

Fig. 6. SEM images of solid materials in the Mg–6Zn–1.5Y–0.5Ce system in the course of extrusion.

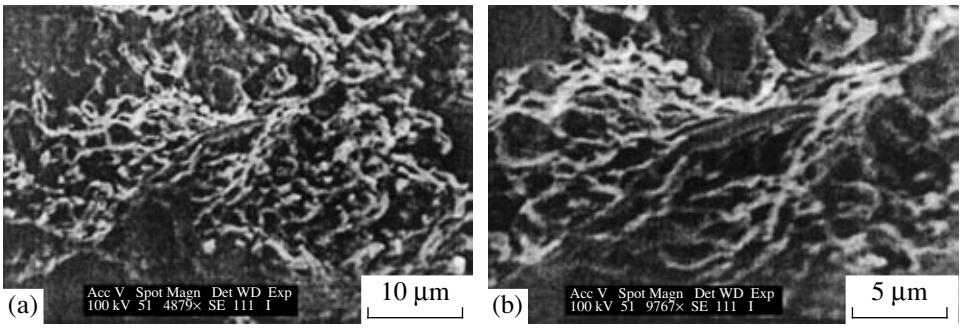

Fig. 7. SEM images of the fractures observed for the Mg–6Zn–1.5Y–0.5Ce samples ruptured under tension in the course of extrusion.

Zn–Y system to be formed. In the Mg–Zn–Y–Ce system, cerium can considerably enhance the redistribution of the solute and, thus, promote the remelting of the arms in the coarse dendritic grains. It is this cerium that favors the formation of the network surrounding the grains and submicroparticles in the grains.

Among the arms of the dendritic segments, the dispersed melt solidifies according to the same mechanism of anomalous eutectic solidification with the formation of dispersed intermetallic submicroparticles as the final product. The finer and denser the dendrite arms and the larger the zones of the dispersed melt, the higher the uniformity of intermetallic submicroparticles. Consequently, the closer the quenching region, the higher the solidification rate, the finer the dendrite arms, and, hence, the denser the submicroparticles. This can be seen in the microstructure of the quenched surface of the Mg–Zn–Y–Ce alloy (Fig. 4).

Mechanism of Strengthening of As-Extruded Solid Materials

Since the extruded solid materials prepared from the rapidly quenched ribbons contain particles incompatible with the matrix, these materials can be considered composites with metal matrices. Therefore, according to Mabuchi and Higashi [17], the mechanism of their strengthening involves the following five processes with the corresponding contributions: (i) the dislocation–particle interaction associated with the Orowan process, $\Delta\sigma_O$; (ii) the load transfer from the matrix to particles, $\Delta\sigma_L$; (iii) the generation of dislocations due to the difference between the thermal expansions of the matrix and particles, $\Delta\sigma_T$; (iv) the generation of dislocations due to the geometric requirements in the course of deformation, $\Delta\sigma_D$; and (v) the fine-grain strengthening, $\Delta\sigma_G$. The strength of the extruded solid material can be represented in the form

$$\Sigma_{0.2} = \Delta\sigma_O + \Delta\sigma_L + \Delta\sigma_T + \Delta\sigma_D + \Delta\sigma_G. \quad (1)$$

The strengthening associated with the Orowan process can be written as follows:

$$\Delta\sigma_O = \frac{0.81MGb\ln(d_p/b)}{2\pi(1-\nu)^{1/2}(\lambda - d_p)}, \quad (2)$$

where M is the Taylor factor (6.5 for Mg), G is the shear modulus (1.66×10^4 MPa for Mg), b is the Burgers vector (3.21×10^{-10} m for Mg), ν is the Poisson ratio, d_p is the diameter of precipitated particles (0.2×10^{-6} m), and λ is the mean distance between the centers of particles (1.0×10^{-6} m). The calculated contribution of the Orowan process to the strength is approximately equal to 78 MPa.

The contribution of the load transfer from the matrix to particles is defined by the relationship

$$\Delta\sigma_L = \sigma_S\left(\frac{1}{2}f_v\right), \quad (3)$$

where σ_S is the yield strength of the matrix (determined by the supersaturated magnesium solid solution) and f_v (25%) is the volume fraction of dispersed particles. Owing to the solute trapping effect, this contribution is no less than 140 MPa and, hence, the contribution of this process is approximately equal to 17 MPa.

The strengthening due to the difference between the thermal expansions of the matrix and particles is given by the formula

$$\Delta\sigma_T = aGb\left(\frac{12\Delta T\Delta C f_v}{bd_p}\right)^{1/2}, \quad (4)$$

where α is a constant, ΔT is the temperature increment, and $\Delta C = C_{Mg} - C_W$ is the difference between the thermal expansion coefficients of the matrix and particles under investigation. At $\alpha = 1.25$, $C_{Mg} = 2.61 \times 10^{-5}$ K, and $C_W = 7.5 \times 10^{-6}$ K, this contribution is estimated at 70 MPa.

The contribution associated with the generation of dislocations due to the geometric requirements during deformation can be written as

$$\Delta\sigma_D = aGb\left(\frac{f_v 8\gamma}{bd_p}\right)^{1/2}, \quad (5)$$

where γ is the shear strain calculated with the use of the Taylor factor. According to [17], this contribution is approximately estimated at 70 MPa.

The fine-grain strengthening ensures the largest contribution to the strength of rapidly solidified magnesium alloys. This contribution can be represented by the Hall–Petch equation

$$\Delta\sigma_G = K/d^{1/2}, \quad (6)$$

where K is a constant (0.28 M nm for Mg) and d is the grain size (~5×10^{-6} m; here, the calculations are performed using ribbon grain diameters and the results is very underestimated). In our case, this contribution is approximately equal to 396 MPa. Such a large contribution is explained by the hexagonal close-packed structure of the material. Armstrong *et al.* established that the constant K in the Hall–Petch equation and the Taylor factor M are related by the expression

$$K \propto M^2\tau_C, \quad (7)$$

where τ_C is the shear stress required for operating a slip source and M depends on the number of slip systems. Since the slip systems are limited in metals with the hexagonal close-packed lattice and the factor M for metals with this lattice is larger than that for metals with the face-centered cubic and body-centered lattices, the strength of the former metals strongly depends on the grain size [17, 18]. Consequently, the decrease in the degree of granularity through rapid solidification is the most promising method for producing magnesium alloys with a high strength (above 500 MPa) [19–23].

According to the mechanisms of strengthening, the sum of all the contributions should be approximately equal to 0.2% of the yield stress or the tensile yield strength [17]. The calculated total contribution is equal to 630 MPa, which is considerably larger than experimental tensile strengths of 490–520 MPa. The discrepancy between the calculated and experimental results can be explained by analyzing the microstructure.

As can be seen from the images of the fractures (Fig. 7), the extruded solid materials possess a high ductility. This is associated with the decrease in the grain size, which enhances the deformation of the matrix and rotation of grains in the course of tension experiments. A higher ductility could be achieved by improving the conditions for welding of the dispersed ribbon particles during extrusion.

The defects of welding between dispersed ribbon particles can be seen in Fig. 6. These defects are formed in the course of extrusion and illustrate the fact that the strength of materials extruded from rapidly solidified ribbons depends on the microstructure of the rapidly solidified powder and extrusion conditions. Any problems at different extrusion stages can lead to lack of success in preparing a high-quality extruded product.

CONCLUSIONS

Alloys in the Mg–Zn–Y–Ce system with an improved microstructure of grains were prepared by two methods, namely, by conventional casting and rapid solidification. The mean sizes of magnesium solid-solution grains and supersaturated magnesium solid-solution grains are equal to 45 and 5 μm for alloys produced by casting and rapid solidification, respectively. The improvement of the grain structure is associated with the remelting of dendrites. In this process, cerium plays an important role due to its limited solubility in magnesium.

High-strength solid products (diameter, 8–50 mm) in the Mg–6Zn–1.5Y–0.5Ce system were obtained by extrusion of powdered, rapidly solidified ribbons. These materials are characterized by tensile strengths of 490–520 MPa and limited elongations.

The expected tensile yield strength of extruded high-strength solid materials in the Mg–6Zn–1.5Y–0.5Ce system is equal to 630 MPa, as judged from the theoretical analysis of their fine structure.

ACKNOWLEDGMENTS

We would like to thank J. Kinstler, L. Glazman, and A. Weiss for preparing the materials. We also acknowledge the support of the Israel Consortium. X. Guo acknowledges the support of the National Natural Sciences Foundation of China.

REFERENCES

1. Baikov, A.A., *Magnievye splavy s ittriem* (Magnesium Alloys with Yttrium), Moscow: Nauka, 1979.
2. Antion, C., Donnadieu, P., Perrard, F., Deschamps, A., Tassin, C., and Pisch, A., Hardening Precipitation in Mg–4Y–3Re Alloy, *Acta Mater.*, 2003, vol. 51, no. 18, pp. 5335–5348.
3. Singh Alok, Nakamura, M., Watanabe, M., Kato, A., and Tsai, A.P., Quasicrystal Strengthened Mg–Zn–Y Alloys by Extrusion, *Scr. Mater.*, 2003, vol. 49, no. 5, pp. 417–422.
4. Ravi Kumar, N.V., Blandin, J.J., Suéry, M., and Grosiean, E., Effect of Elements on the Ignition Resistance of Magnesium Alloys, *Scr. Mater.*, 2003, vol. 49, no. 3, pp. 225–230.
5. Singh Alok and Tsai, A.P., On the Cubic W Phase and Its Relationship to the Icosahedral Phase in Mg–Zn–Y Alloys, *Scr. Mater.*, 2003, vol. 49, no. 2, pp. 143–148.
6. Avedesian, M.M. and Baker, H., *Magnesium and Magnesium Alloys*, Materials Park, Ohio: The Materials Information Society, 1999, pp. 15–20, 53–77.

7. Kubota, K., Mabuchi, M., and Higashi, K., Processing and Mechanical Properties of Fine-Grained Magnesium Alloys, *J. Mater. Sci.,* 1999, vol. 34, no. 10, pp. 2255–2262.
8. Froes, F.H. and Ward-Close, C.M., Processing of Light Metals for Enhanced Performance, *J. Mater. Proc. Technol.*, 1995, vol. 48, pp. 667–673.
9. Krishnamurthy, S., Robertson, E., and Froes, F.G., Rapidly Solidified Magnesium Alloys Containing Rare Earth Additions, in *Advances in Magnesium Alloys and Compositions*, Paris, H. and Hunt, W.H., Eds., The Minerals, Metals, and Materials Society, 1988, pp. 77–88.
10. Jackson, K.A., Seward, T.P., *et al.*, On the Origin of the Equiaxed Zone in Castings, *Trans. Metall. Soc. AIME,* 1966, pp. 149–158.
11. Nayeb-Hashemi, A.A. and Clarc, J.B., in *Phase Diagrams of Binary Magnesium Alloys, Metals Park, Ohio: ASM International*, 1988, pp. 878–880.
12. Aziz, M.J., Model for Solute Redistribution: During Rapid Solidification, *J. Appl. Phys.*, 1982, vol. 53, no. 2, pp. 1158–1168.
13. Boettinger, W.J., Coriell, S.R., and Trivedi, R., in *Rapid Solidification Processing: Principle and Technologies IV*, Mehrabian, R. and Parrish, P.A., Eds., Baton Rouge, LA: Claitor, 1988, p. 13.
14. Willnecker, R., Herlach, D.M., and Feuerbacher, B., Evidence of Nonequilibrium Processes in Rapid Solidification of Undercooled Metals, *Phys. Rev. Lett.*, 1989, vol. 62, no. 5, pp. 2707–2710.
15. Kattamis, T.Z. and Flemings, M.C., Dendrite Structure and Grain Size of Undercooled Melts, *Trans. Metall. Soc. AIME*, 1966, vol. 236, pp. 1523–1532.
16. Wu, Y., Piccone, T.J., Shiohara, Y., and Fleming, M.C., Dendritic Growth of Undercooled Nickel–Tin: Part I, *Metall. Trans. A*, 1987, vol. 18, pp. 915–924; Piccone, T.J., Wu, Y., Shiohara, Y., and Fleming, M.C., Dendritic Growth of Undercooled Nickel–Tin: Part II, *Metall. Trans. A*, 1987, vol. 18, pp. 925–932.
17. Mabuchi, M. and Higashi, K., Strengthening Mechanisms of Mg–Si Alloys, *Acta Mater.*, 1996, vol. 44, no. 11, pp. 4611–4618.
18. Lucac, P., Synergetic Effects in Simultaneous Strengthening and Plasticizing of Magnesium Based Alloys, in *Proceedings of the 1th Israel Conference on Magnesium Science and Technology "Magnesium-97,"* Aghion, E. and Eliezer, D., Eds., Beer-Sheva, 1997, p. 139–144.
19. Shaw, C. and Jones, H., Structure and Mechanical Properties of Two Mg–Al–Ca Alloys Consolidated from Atomized Powder, *Mater. Sci. Technol.*, 1999, vol. 15, pp. 78–84.
20. Shibata, T., Kavanishi, J., Nagahora, J., Inoue, A., and Masumoto, T., High Specific Strength of Extruded Mg–Al–Ge Alloys Produced by Rapid Solidification Processing, *Mater. Sci. Eng., A*, 1994, vols. 179–180, pp. 632–636.
21. Miyazaki, T., Kaneko, J., and Sugamata, M., Structures and Proportions of Rapidly Solidified Mg–Ca Alloys, *Mater. Sci. Eng., A*, 1994, vols. 181–182, pp. 1410–1414.
22. Shaw, C. and Jones, H., The Contributions of Different Alloying Additions in Rapidly Solidified Magnesium Alloys, *Mater. Sci. Eng., A*, 1997, vols. 226–228, pp. 856–860.
23. Kato, A., Horikiri, H., Inoue, A., and Masumoto, T., Microstructure and Mechanical Properties of Bulk $Mg_{70}Ca_{10}Al_{20}$ Alloys Produced by Extrusion of Atomized Powders, *Mater. Sci. Eng., A*, 1994, vols. 179–180, pp. 707–711.